Vibrated powders: Structure, correlations, and dynamics

G. C. Barker
Theory and Computational Science Group, AFRC Institute of Food Research, Colney Lane, Norwich NR4 7UA, United Kingdom

Anita Mehta
Theory of Condensed Matter Group, Cavendish Laboratory, Madingley Road, Cambridge CB3 0HE, United Kingdom
*and Interdisciplinary Research Center in Materials for High-Performance Applications, University of Birmingham, Edgbaston, Birmingham B15 2TT, United Kingdom**

(Received 13 September 1991)

The structure and dynamics of powders subjected to vibration are investigated by a nonsequential and cooperative computer-simulation approach in three dimensions. Starting from a microscopic model of the physics, we are able to probe independent and collective effects in the dynamics of vibrated powders, as well as in the resulting structures. In particular, we analyze the role of cooperative structures such as bridges, which are always present in reality and which cannot be formed by purely sequential processes. We look in depth at the behavior of the volume fraction and coordination number as a function of the intensity of vibration, as well as at correlation functions describing contacts between neighboring grains, also as a function of intensity. Satisfying agreement with the qualitative predictions of earlier analytic work is obtained, and a framework is laid for future investigations.

PACS number(s): 05.40.+j, 05.60.+w, 81.90.+c, 82.70.−y

I. INTRODUCTION AND AN OUTLINE OF THE MODEL

Powders are materials that are composed of dense collections of solid grains. They vary in their composition, ranging from coarse-grained aggregates to fine-grade powders; in their packing, ranging from loosely to close-packed states; and in their states of motion, ranging from stationary piles to continuous flowing masses. They have been of interest to engineers [1,2] for a long time, but it is only recently that they have become an important and exciting area of theoretical [3–9] and experimental [10–13] physics.

Powders exhibit behavior that is neither completely solidlike nor completely liquidlike, but intermediate between the two. In addition to phenomena exhibited by other amorphous systems, their randomness of shape and texture strongly influences their static and dynamic properties. They are highly nonlinear and hysteretic, as a consequence of which they show complexity, so that the occurrence and relative stability of a large number of metastable configurations govern their behavior. Finally, a unique feature of granular materials is that they show dilatancy [1], which is the ability to sustain different degrees of packing.

However, the subjects of this paper are those features of the static and the dynamic properties of granular materials that are *universal*, i.e., that do not depend on the details of the particle sizes or on the material properties of the individual grains. Examples of such properties are the existence of a fixed maximum random-packing fraction or the size segregation induced by shaking. In order to investigate such characteristic granular behavior we have investigated a model powder that is made from monodisperse, hard spherical grains so as to highlight the (generic) microscopic behavior of the grains, and the way that this influences the macroscopic physics of granular materials. We have used a three-dimensional computer-simulation method to obtain microscopic details of the grain configurations and to probe the independent-particle and the collective effects that occur within a vibrated bed of grains. We present here an extended account of previous work [9], in which we investigate phenomena that contribute to the behavior of dry powders.

Thermal agitation in a powder takes place on an atomic rather than a particulate scale; therefore it is external vibrations that play an essential role in the behavior of powders. In the absence of external agitation, the grains are frozen into one configuration (since their thermal energy is insufficient to generate the equivalent of Brownian motion), which represents one of the many possible *metastable* states of the system—we note in passing that this is one of the reasons why powders show *complexity*. In the microscopic model [3], on which this work was based (a quantitative version of which is presented elsewhere [8]), a granular pile is represented by an assembly of potential wells, each representing a local cluster of grains, while the effect of vibration applied to the pile is modeled as being an effective noise H. If H is greater than the binding energy of the particles to their clusters, then the grains are ejected, and move into neighboring clusters; in terms of the real powder, this means that grains are ejected individually (*independent-particle relaxation*) from their clusters. Conversely, if H is small relative to the binding energies of the particles, they are not ejected; this energy goes into the reorganization of the grains (*collective relaxation*) within their clusters to minimize voids. The claim is [3,8] that for high intensities of vibration, the dominant process is single-particle relaxation, whereas collective relaxation dominates at low intensities.

It will be realized that while single-particle relaxation leads to a rapid decay of the slope, it will lead to a low packing fraction and a rough surface. Equally, when collective relaxation dominates, the slope will relax slowly or not at all; on the other hand, slow collective reorganization of particles will lead to efficient void filling, i.e., to a high packing fraction and a smooth surface. We have in earlier work [4] investigated the phenomenon of granular relaxation in relation to the decay of the slope of a sandpile subjected to vibration, and will focus here on the effect of the relaxational dynamics on the structure of the powder and the correlations within it.

II. A SURVEY OF REORGANIZATION SCHEMES: THE PHILOSOPHY UNDERLYING OUR OWN

The static powder is only characteristic of the method of preparation—thus demonstrating *hysteresis;* and an ensemble of configurations, built from independent realizations of the whole powder using the same method, is representative of a particular aggregation method. Many aggregation schemes have been investigated in this way, including the deposition model of Vold [14], ballistic deposition [15], close packing with surface restructuring [16], and diffusion-limited aggregation [17]. Of these schemes, the simplest is the Vold model, in which particles stick instantaneously on impact. In ballistic deposition, no trajectories are computed, and aggregation sites are chosen from a list, while in diffusion-limited aggregation, random-walk trajectories precede the aggregation phase. In all these cases, the initial choice of a site terminates the process, i.e., particles stick on impact. The model of Ref. [16] goes further, in that particles are allowed to roll around after impact on a *stationary* aggregate until they find a local minimum of potential energy, but this is *still* a sequential process. In contrast, the schemes developed here and elsewhere [4,9] contain collective restructuring, where the aggregate restructures simultaneously with the incoming particles, thus making our process *nonsequential and cooperative,* and therefore capable of incorporating realistic reorganization processes. This essential ingredient makes our methods much more reflective of many-particle events in a moving granular system.

When mechanical energy is supplied to a powder, in the form of stirring, shaking, or conveying operations, periods of release are introduced. During the periods of release, the grains have some freedom to rearrange their positions relative to their neighbors, and the powder "jumps" [3] between different, but related, grain configurations. In this case a series of grain configurations represents the dynamic response of the powder to forcing excitations. In general, this response has both transient and steady-state components. Thus a shaken powder follows a path through the phase space of powder configurations, which depends on both the dynamics of the individual grains and on the intensities and frequencies of the component vibrations of the driving force.

In practice, qualitatively similar driving forces may result in rather different behavior in the powder. Thus vibrations are frequently used to enhance powder mixing, whereas, in contrast, they may also be identified as a source of size-segregation effects [18–20]. Similarly, slow shaking, or "tapping," may be used as a means of powder compaction, especially after a pouring process, but agitated powders can also be significantly more fluid than their unshaken counterparts. Our aim is to distinguish, in terms of individual and collective relaxations [9], the different microscopic responses that underlie the macroscopic response of a powder subject to vertical vibrations at different intensities. In our simulation model [4,9], the driving force is periodic, and leads to clearly defined periods of dilation of the powder assembly, between which we have static configurations of grains. The driving force is applied uniaxially and is coupled homogeneously to the powder, so that free volume is introduced uniformly. During the periods of dilation the grain motion is dominated by a strong uniaxial gravitational field and by hard-core interactions with neighboring particles and the container base.

For a noncohesive powder, it is clear that stirring, shaking, and pouring are all many-particle operations. During these processes the particles follow complicated trajectories, composed of free-fall segments punctuated by hard, inelastic collisions with the other particles before they reach stable positions in a static assembly. These trajectories are fundamentally nonsequential, that is, the route of one particle to its stable position cannot be computed without simultaneously computing the routes of many other particles. Stable configurations are those in which each particle rests in a potential-energy minimum, and therefore cannot lower its potential energy any further by local or nonlocal motion. In practice, this means that each particle is in contact with at least three others.

The static configurations of grains that result from shaking reflect the essentially nonsequential nature of the process. These configurations contain particle bridges [4,9] and a wide variety of void shapes and sizes that do not occur in sequentially deposited aggregates. In this context, a bridge is a stable arrangement of particles in which at least two of the particles depend on each other for their stability. Bridges cannot be formed by the sequential placement of particles into stable positions but are a natural consequence of the simultaneous settling motion of closely neighboring particles. In our simulations [9] we have approximated the precise particle trajectories by using a low-temperature Monte Carlo method supplemented by a nonsequential random-close-packing algorithm. This is a compromise. At the expense of losing information concerning the granular dynamics, we can efficiently produce static structures that correspond to a nonsequential deposition process. Previous simulations [15,16] have failed to build in this aspect of shaking.

Our method falls between authentic granular-dynamics simulations [21,22] and previous shaking simulations [15], which combine sequential deposition with a search for global minima of the potential energy. Visscher and Bolsterli [15] have performed computer simulations of vibrated beds of hard spheres; they have, however, interpreted the shaking process only in terms of its outcome,

i.e., in terms of the final, static configurations of the grains. Their shaken grain configurations were built, using an adapted random-close-packing procedure; that is, by adding grains one by one at sites of minimum potential energy chosen from a set of trial random-close-packing sites. The resulting packings, which remain fully sequential, have volume fractions $\phi \cong 0.60$, which are greater than those for unshaken configurations but still significantly below the maximum volume fraction for random close packing of $\phi = 0.64$ [23]. More recently, Rosato *et al.* [24] introduced a two-dimensional Monte Carlo method to study the size segregation that is induced by shaking. Their method includes important nonsequential features but does not include a criterion for the stability of the packing, and hence cannot be used, directly, to follow the changes in volume fraction or particle coordinations that occur as a result of applied vibrations. In a three-dimensional simulation, Soppe [25] produced nonsequential consolidated packings by combining a Monte Carlo compression with ballistic deposition. This method also omits an explicit stability criterion, but, by using a particular prescription for annealing the packing, it leads to unstable beds of particles with volume fractions $\phi \cong 0.60$. Stable packings that contain features due to nonsequential reorganization were used by Duke, Barker, and Mehta [4] to study the steady relaxation of the slope of a two-dimensional pile of hard particles that is caused by vertical vibrations. These simulations reproduced qualitative features of the relaxation and indicated that collective particle motions, over length scales comparable with the nonsequential structural components, were important. This method forms an integral part of the shaking simulations presented below.

Granular-dynamics simulations are usually performed in one of two distinct regimes. First there is a grain-inertial regime [21,22], in which instantaneous, inelastic two-particle collisions dominate the motion. These simulations model powders under highly energetic (kinetic) flow conditions, and they are most efficient at moderate particle densities of $\phi \cong 0.3-0.4$. In may ways, the implementation of granular dynamics in the grain-inertial regime follows the standard methods established for the molecular dynamics of complex fluids using collections of rough hard spheres. However, one important distinction arises because the collisions between particles, unlike those between molecules, are inelastic. The second granular-dynamics regime, called the quasistatic regime, is used to model [26] the slow, collective motion of close-packed ($\phi \geq 0.55$) collections of particles. In this case, the contact forces between two particles are most important, and the organization of computer simulations revolves around the efficient solution of many simultaneous equations of motion for interacting particles. For most real materials, the precise nature of the contact forces is unclear—the so-called principles of limiting friction and indeterminacy of stress [2], which are familiar to chemical engineers [27], say that the internal stress in a granular assembly is indeterminate, because the friction between two grains in contact can lie anywhere between zero and a limiting value. Therefore the applications of granular dynamics in the quasistatic regime [26] are restricted by *(ad hoc)* estimates of contact forces usually constructed from viscous and harmonic elements. Most shaking processes take place in a series of regimes that traverse the spectrum from grain inertial to quasistatic, and therefore "shaking" is difficult to simulate with a continuously tuned granular-dynamics prescription. Thus, during a cycle of a shaking process, the grains may experience local particle densities that vary from $\phi \cong 0.3-0.6$ and may go through periods of rapid motion as well as through periods of slow relaxation. We hope to report granular-dynamics simulations of shaking elsewhere, but here we shall introduce a hybrid technique.

Before describing the details of our method, we would like to comment on a few other approaches. Cellular automata [28] are being used increasingly to model granular flow; while these are powerful tools, both because of their flexibility and their relative speed, they are limited by their lattice-based formulation. They are thus good for qualitative descriptions of powder flow, but cannot probe detailed particulate structure during and after flow. The kinetic-theory-type approaches of Haff [29] and Jenkins and Savage [30] and the hydrodynamic approaches of Jackson [31] are appropriate for the situation of rapid shear, where the grains are in constant motion, and the assembly is assigned a "granular temperature" determined by the average mean-square velocity of the grains. These methods are, however, inappropriate for the situation where the grains are in slow, or no, motion with respect to each other—the continuum approach fails, because the discreteness of the grains and the effects of friction and restitution at individual collisions become increasingly important. Our method [9], on the other hand, is able to probe details of particulate structure; in addition, we do not assume a continuum basis or a single granular temperature, and are therefore able to cope better with the quasistatic regime of slow shear.

III. DETAILS OF OUR SIMULATION TECHNIQUE

In our simulations we have a bed (Fig. 1) of monodisperse, hard spheres above a hard, impenetrable, plane

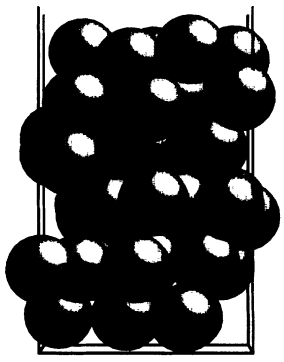

FIG. 1. Schematic diagram of the geometry of the simulation. Hard particles form a periodic bed above an impenetrable base: the diagram shows the primary simulation cell, which is repeated in two perpendicular directions.

base that is at $z=0$. The particle bed is periodic, with a repeat distance of L sphere diameters, in two perpendicular directions, x and y, in the plane. Each primary simulation cell contains N spheres. A unidirectional gravitational field acts downwards, i.e., along the negative-z direction.

Initially, the spheres are placed in the cell using a sequential random-close-packing procedure [32]. The spheres are introduced, one at a time, from large z and at random lateral positions, and follow complex paths, which are composed of vertical line segments and circular arcs, until they reach stable positions in contact either with three other spheres or with the hard base. These sphere trajectories correspond to rolling motions separated by periods of free fall. In this sequential deposition, the moving sphere rolls over spheres that are already located in stable positions; that is, incoming spheres cannot disrupt the stable packing, and they cannot interfere with other aggregating particles. In this sense, the aggregation is slow, and the gravitational field is strong. Many authors have analyzed the sequential, close-packed arrangements of spheres [15,23,33] that are obtained using this procedure. For monodisperse spheres there are boundary layers that extend for approximately five sphere diameters both above the hard base and below the free surface. These layers contain quasiordered arrangements of spheres. Apart from this, the packing is homogeneous with a mean volume fraction $\phi_0=0.581\pm.001$ and a mean sphere coordination $c_0=6.00\pm0.02$ [34]. These values are not altered substantially by introducing a small amount ($\sim 5\%$) of polydispersity, and they adequately describe the packings that are used as initial configurations for our shaking simulations.

In our simulations, the packing is subject to a series of nonsequential, N-particle reorganizations. Each reorganization is performed in three distinct parts: first, a vertical expansion or dilation: second, a Monte Carlo consolidation; and finally a nonsequential close-packing procedure. We shall call each full reorganization a shake cycle or, simply, a shake. The duration of our model shaking processes and the lengths of other time intervals are conveniently measured in units of the shake cycle.

The first part of the shake cycle [4,9] is a uniform vertical expansion of the sphere packing, accompanied by random, horizontal shifts of the sphere positions. Sphere i, at height z_i, is raised to a new height $z_i'=(1+\epsilon)z_i$. For each sphere, new lateral coordinates are assigned, according to the transformation $x'=x+\xi_x$, $y'=y+\xi_y$, providing they do not lead to an overlapping sphere configuration; here ξ_x and ξ_y are Gaussian random variables with zero mean and variance ϵ^2. The expansion introduces a free volume of size ϵ between the spheres and facilitates their cooperative rearrangement during phases 2 and 3 of the shake cycle. This expansion is *virtual:* we seek merely to introduce a free volume, not to model a physical expansion. The parameter ϵ is a measure of the intensity of vibration; although we do not know the exact functional relationship between these two quantities, we expect them to vary monotonically for reasonably small ϵ. We have assumed that the freedom of motion of the particles in the interior of the packing increases with the intensity of the applied vibrations.

In the second phase of the cycle, the whole system is compressed by a series of displacements of individual spheres. Spheres are chose at random and displaced according to a very-low-temperature, hard-sphere, Monte Carlo algorithm. A trial position for sphere i is given by $\mathbf{r}_i'=\mathbf{r}_i+\mathbf{a}d$, where $\mathbf{a}$ is a random vector with components $-1\le a_x,a_y,a_z\le 1$, and d defines the size of a neighborhood for the spheres. The move is accepted if it reduces the height of sphere i without causing any overlaps. All the successful moves reduce the overall potential energy of the system. The process continues until the efficiency with which moves are accepted, measured by batch sampling, falls below a threshold value e. Here d and e are free parameters that are chosen to optimize the computational method. It is shown below that there is a regime in which the static results are not strongly dependent on this choice.

Finally, the sphere packing is stabilized using an extension of the random-close-packing method described above. The spheres are chosen in order of increasing height and, in turn, are allowed to roll and fall into stable positions. In this part of the shake cycle spheres may roll over, and rest on, any other sphere in the assembly. This includes those spheres that are still to be stabilized and that may, in turn, undergo further rolls and falls. In this way, touching particles can be continually moved until no further rolling is possible. This procedure allows the formation of complex, stable, structural components, like bridges and arches, which *cannot* be constructed by purely sequential processes [4,9].

The outcome of a shake cycle is to replace one stable close-packed configuration by another. In these configurations, each particle occupies a cluster that is formed by its neighbors, and a "shake" is thus a reorganization scheme for a set of clusters. The role of the individual parts of the shake cycle is clear. Expansion represents a challenge of variable degree to the integrity of the clusters. The Monte Carlo compression reinstates those clusters that were deformed and, when necessary, creates new clusters where the previous ones were destroyed. Finally, the stabilization phase positions the particles inside the set of clusters established in phase 2. In phase 2, the Monte Carlo procedure generates a time-ordered sequence of states that culminates with a state that has an isolated potential well for each particle. Although this does not replicate at every instant the actual dynamical processes that lead to the static configuration of spheres, and the dynamical information that it contains will depend on the choices for d and e, it seems reasonable that the set of clusters that is produced is not too sensitive to these details.

In practice, during phase one of the nth shake cycle, the mean volume fraction of the assembly falls from ϕ_{n-1} to $\phi_{n-1}/(1+\epsilon)$. In phase 2 the volume fraction steadily increases to $\phi_n\cong\phi_{n-1}$, and in phase 3 it remains approximately constant. In contrast, the mean coordination number is reduced from c_{n-1} to zero in the expansion phase of the nth shake and remains zero throughout the Monte Carlo compression, but, during stabilization, it increases steadily to $c_n\cong c_{n-1}$.

IV. SOME COMMENTS ON THE TRANSIENT REGIME, AND STEADY-STATE RESULTS

The continuous evolution of particle positions and velocities that occurs during a physical shaking process is replaced, in our simulations, by a time-ordered, discrete set of static N-particle configurations. The members of each set are the nonsequentially reorganized close packings that are obtained after integral numbers t of completed shake cycles starting from a sequential random close packing. Each set of configurations may be labeled by three parameters e, d, and ϵ. For each member of these sets we have evaluated "material" properties, such as the volume fraction and the mean coordination number, from the central portion of the packing in order to minimize the surface effects. In all cases, this volume contains more than 50% of the spheres in the simulation cell.

A. Volume fractions and coordination numbers

Figure 2 shows the variation of the volume fraction ϕ with the number of shakes t for two different shaking intensities $\epsilon=0.05$ and 0.5. In both cases $e=d=0.01$, $N=1300$, and $L=8$ particle diameters. At low intensity, the volume fraction increases slowly for $t<50$ and fluctuates around a steady value, $\phi=0.598\pm.003$, at larger times. This corresponds to a slow compaction towards a vibrational steady state. In this state nonsequential reorganizations of intensity $\epsilon=0.05$ leave the volume fraction of the packing substantially unaltered. The steady state does not depend on the particular choice of starting configuration or on particular sets of pseudorandom numbers used during the shake cycles. For $\epsilon=0.5$, the evolution of the volume fraction of the packing is more complicated. The first two shake cycles significantly reduce the volume fraction of the packing from that of the sequential deposit to $\phi=0.562\pm0.002$. Following this there is another transient period, $t<30$, in which the volume fraction partially recovers. Finally, for $t>40$ another vibrational steady state is achieved, with $\phi=0.569\pm0.002$.

Thus, over a range of shaking intensity, repeated nonsequential reorganization leads to packings with bulk properties that are insensitive to further vibrations. The properties of the vibrational steady states will be discussed, in detail, below. Results have been obtained by taking averages from sets of m consecutive configurations in the steady-state shaking regime with $m\cong50$. Throughout, we have used simulations with $N\cong1300$ and $L=8$ particle diameters, for which the mean depth of the packing is approximately 20 particle diameters. For shallower packings, the measured volume fractions are too large. This is because the hard base at $z=0$ causes some ordered, denser regions to occur in the lowest layers of the packing. These layers are unimportant when measuring the volume fractions of packings with depths greater than ten particle diameters. We have also tested the dependence of the volume fraction on the cell size L for fixed bed depths, and conclude that serious size dependence is absent for $L\geq8$.

Monte Carlo consolidation is, structurally, the most influential, and computationally the most intensive part of each shake cycle. The duration of this phase, which can be measured in terms of the number of Monte Carlo steps per particle N_{MC}/N, can be increased either by decreasing e (the terminating efficiency of the Monte Carlo sequence) or by decreasing d (the maximum size of each Monte Carlo step). However, the results of hybrid simulations are not related trivially to the details of the Monte Carlo component alone. In Fig. 3 we have plotted, for several values of d, the steady-state volume fraction ϕ against the length of the Monte Carlo consolidation. Each data point in Fig. 3 has been obtained from a separate simulation, with $\epsilon=0.5$, $N\cong1300$, and $L=8$ particle diameters, by averaging the volume fraction over 20 consecutive steady-state shaking configurations. Most importantly, for long Monte Carlo consolidations, i.e., for sufficiently small values of e, the volume fraction data collapses onto a single, constant value that is independent of d.

Figure 3 shows that, in the absence of the Monte Carlo

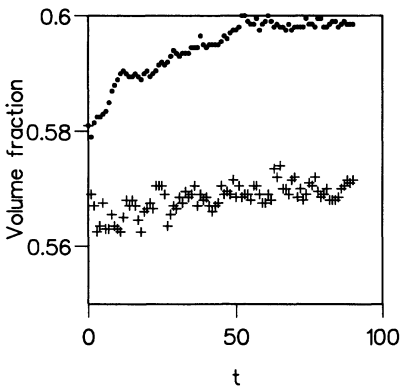

FIG. 2. Volume fraction of monodisperse hard spheres plotted against the number of cycles t, of a computer-simulated shaking process. The initial state is a sequential random close packing, with volume fraction 0.581, and the shaking intensity is $\epsilon=0.05$ (●) and 0.5 (+).

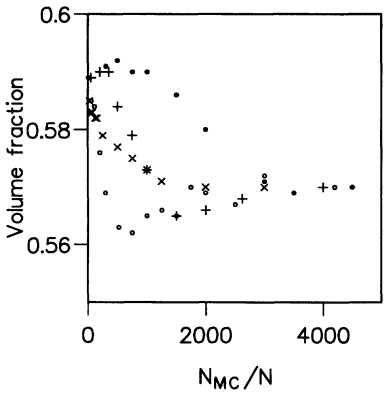

FIG. 3. Steady-state volume fraction of monodisperse hard spheres plotted against the length of Monte Carlo consolidation (measured in Monte Carlo steps per particle N_{MC}/N). The Monte Carlo consolidation is the second phase of a three-phase computer-simulated shaking process with shaking intensity $\epsilon=0.5$. The maximum Monte Carlo step lengths are $d=0.004$ (●), 0.01 (+), 0.05 (○), and 0.2 (×).

phase, the steady-state volume fraction, for shaking intensity $\epsilon=0.5$, is $\phi=0.589\pm0.001$. This is greater than the volume fraction for a sequential deposition process, which itself could be viewed as a shaking process, without a Monte Carlo phase, of intensity $\epsilon=\infty$. For the smallest values of d, the Monte Carlo consolidation has little effect for $N_{MC}/N<10^3$. This indicates that, in the first part of the Monte Carlo dynamics, the particles experience a period of free diffusion. For longer consolidations, and for larger values of d, the downward motion of the particles is a collective process. The regions of Fig. 3 in which ϕ decreases with N_{MC}/N correspond to increased numbers of cooperative features that are trapped into the stable, close-packed structure by extending the period of Monte Carlo consolidation. The minima in Fig. 3 indicate that premature termination of the Monte Carlo consolidation can cause too many large bridges and voids to be trapped in the stable packing. The mean coordination number of the spheres c remains weakly dependent on d for long Monte Carlo consolidations, but, in tests with $\epsilon=0.05$ and 0.5, the values of c obtained by extrapolation to $d=0$ do not differ substantially from those obtained with $d=0.01$.

After the above comments on the transient regime, we now discuss the steady state: the results presented in the following are mean values taken from $m\cong50$ consecutive cycles in the steady-state regime of the shaking process. Figure 4 shows the variation of the steady-state volume fraction ϕ with the intensity of vibration ϵ. For $\epsilon>1.0$, the volume fraction is only weakly dependent on ϵ with $\phi\cong0.550\pm0.003$. However, ϕ rises sharply as ϵ is reduced below $\epsilon=1.0$ and, for $\epsilon\leq0.2$, the shaken assembly adopts configurations that are more compact than those for sequentially deposited spheres. This is a clear manifestation of the collective nature of the structures that are introduced by a shaking process.

Figure 5 shows the variation of the steady-state mean coordination number of the spheres c with the intensity of vibration ϵ. For $\epsilon\leq0.25$, the mean coordination decreases as ϵ increases, and it is approximately constant at $c\cong4.48\pm0.03$ for larger intensities. The mean coordination number in a shaken assembly is substantially below that for a sequential deposit ($c\cong6.0$) reflecting the presence of bridges and other void-generating structures.

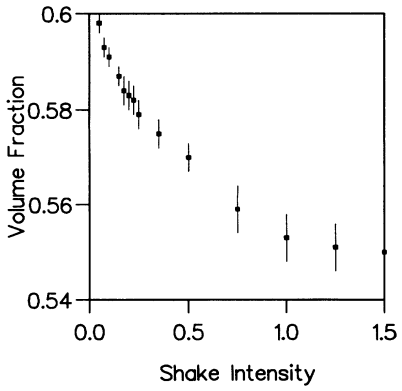

FIG. 4. Steady-state volume fraction of monodisperse hard spheres plotted against the shaking intensity.

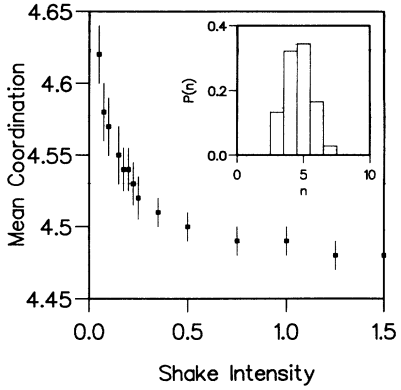

FIG. 5. Mean coordination number of monodisperse hard spheres plotted against the shaking intensity. The inset shows the mean fractions $P(n)$ of spheres that are n-fold coordinated in the steady-state regime of the shaking process that has shaking intensity $\epsilon=0.05$ (solid lines) and 0.5 (dashed lines).

Also shown in Fig. 5 are the mean fractions, $P(n)$ for $n=3-9$, of spheres that are n-fold coordinated in packings subjected to steady-state shaking vibrations at intensities $\epsilon=0.05$ and 0.5. Most spheres touch four or five of their neighbors. For larger values of ϵ, the proportion of fourfold-coordinated spheres is increased, largely at the expense of sixfold-coordinated spheres; i.e., the peak of the distribution moves towards lower coordination numbers.

From Figs. 4 and 5 we note that for $0.25\leq\epsilon\leq1.0$, the steady-state volume fraction steadily decreases with ϵ, while the mean coordination number remains constant. This is consistent with the interpretation that, on the one hand, the density of bridges is independent of ϵ, but that, on the other, the shapes of the bridges become in general more eccentric (and therefore more wasteful of space) as ϵ is increased.

B. Network analysis

Each stable configuration of spheres has associated with it a network, called the contact network, which can be formed by drawing line segments between the centers of all pairs of touching spheres. We have studied the evolution of the contact network in order to follow local sphere correlations during shaking. For each sphere i at time t we define an $(N-1)$-dimensional vector $\mathbf{b}_i(t)$, such that the jth element of $\mathbf{b}_i(t)$ is unity if sphere i is touching sphere j at time t, and zero otherwise. Figure 6 shows the variation with time of the average autocorrelation function

$$z(t)=\langle \mathbf{b}_i(t')\cdot\mathbf{b}_i(t+t')/|\mathbf{b}_i(t')||\mathbf{b}_i(t+t')|\rangle ,$$

for spheres in the interior of the packing, at two shaking intensities $\epsilon=0.05$ and 0.5. In both instances the initial rate of breaking of contacts is greatest, and for larger times $t\geq10$ the rate becomes approximately constant. The main conclusion from the figure is that contact correlations disappear relatively slowly for low intensities of vibration: more quantitatively, we find that a single nonsequential reorganization with $\epsilon=0.5$ is approximate-

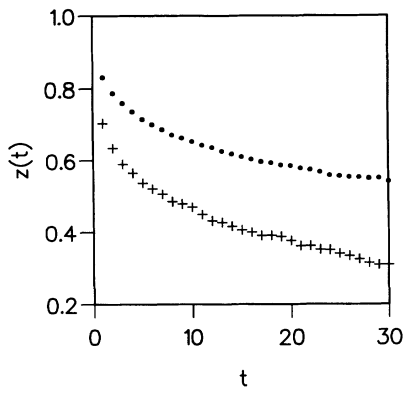

FIG. 6. Autocorrelation function $z(t)$ of the contact network plotted against the number of shake cycles t for monodisperse hard spheres in the steady-state regime. The shaking intensity is $\epsilon=0.05$ (●) and 0.5 (+).

ly twice as efficient at disrupting the contact network as one with $\epsilon=0.05$.

The behavior of $z(t)$ is consistent with snapshot observations of consecutive contact network configurations. Figure 7 highlights the responses of a small group of neighboring spheres, which are in the interior of a much larger packing, to vibrations of two different intensities. Figure 7(a) shows the spheres that are instantaneously within a spherical capture volume, and Fig. 7(b) shows the contacts between them. We note that contacts between spheres at the periphery of the capture volume and spheres that are outside it are not represented in Fig. 7. The capture volume is centered on sphere A and has a radius of approximately two sphere diameters. In Figs. 7(b)–7(d) small balls mark the positions of centers of the close-packed spheres, and rods represent the sphere contacts. The initial configuration of packed spheres, which is a configuration obtained at the end of one particular shake cycle in the steady-state shaking regime with $\epsilon=0.05$, is shown in Fig. 7(a), and its associated contact network is shown in Fig. 7(b). Figures 7(c) and 7(d) are the contact networks for configurations that are obtained after the application of one further complete shake cycle, with intensity $\epsilon=0.05$ and 0.5, respectively.

In the initial configuration sphere A rests on spheres B, C, and D, and is touched by one other sphere, labeled E, which rests on it. After an additional shake cycle with $\epsilon=0.05$, the sphere A remains stabilized in the same way but has gained a further contact, with sphere F, from above. There are many differences between the networks in Figs. 7(b) and 7(c) but they are mainly small changes, of the sphere positions and the rod orientations, which do not grossly alter the network connectivity. During the extra shake cycle, one sphere has left the capture volume and another has entered it, so that the numbers of centers in Figs. 7(b) and 7(c) are identical. The overall impression is one of network deformation.

In contrast, the network in Fig. 7(d) does not closely resemble the one in Fig. 7(b). There is a net loss of two spheres from the capture volume during the additional shake cycle with $\epsilon=0.5$. After this extra shake, sphere A retains only two of its original supporting neighbors and gains a new one, sphere G. In this case, the overall impression is one of network disruption. The network connectivity is altered significantly in this case, and a comparison of Figs. 7(b) and 7(d) shows many examples of bond creation and annihilation.

A notable insight to be gained from Figs. 7(b)–7(d) is that bridge collapse occurs more frequently for large vibrations. In Fig. 7(b), spheres H and I rest on, and support, each other and therefore form part of a bridge; this feature is retained in Fig. 7(c) (contact network after small vibrations), but not in Fig. 7(d) (contact network after large vibrations), where sphere H gains additional support by contacting sphere A from above. We see from a comparison of Figs. 7(b) and 7(d) that the bridge incorporating spheres H and I has collapsed after a single (large-intensity) shake.

C. Correlation functions

The pair distribution functions of particle positions, $h(r)$ for separations in a horizontal plane and $g(z)$ for separations in the vertical direction, are illustrated in Fig. 8 for $\epsilon=0.05$ and 0.5. The data sets for these functions were collected, over $m\cong 25$ cycles, from horizontal slabs with a thickness of one sphere diameter and from vertical cylinders with cross sections equal to that of one sphere. In both directions, the structure is similar to that expected for dense, hard-sphere fluids. The short-range order is most pronounced in the horizontal direction, while the pair distribution function in the z direction, $g(z)$, is relatively insensitive to variations of the shaking intensity. Both functions indicate the presence of a second shell of neighbors at a separation of approximately two particle diameters: we conclude from these figures that the short-range order decreases with increasing intensity of vibration, in accord with intuition.

During a shake cycle, each particle i is shifted in position by $\Delta\mathbf{r}_i=\Delta x_i\mathbf{i}+\Delta y_i\mathbf{j}+\Delta z_i\mathbf{k}$, where $\mathbf{i}$, $\mathbf{j}$, and $\mathbf{k}$ are unit vectors in the x, y, and z directions. We have plotted, in Fig. 9, correlation functions of the vertical components of displacement Δz_i for $\epsilon=0.05$ and 0.5. $H(r)$ measures the correlations in a horizontal plane and $G(z)$ measure the correlations in the vertical direction according to

$$H(r)=\langle \Delta z_i \Delta z_j \delta(|t_{ij}|-r)\Theta(|z_{ij}|-\tfrac{1}{2})\rangle / \langle |\Delta z_i|\rangle^2 ,$$

$$G(z)=\langle \Delta z_i \Delta z_j \delta(|z_{ij}|-z)\Theta(|t_{ij}|-\tfrac{1}{2})\rangle / \langle |\Delta z_i|\rangle^2 ,$$

where $t_{ij}^2=(x_i-x_j)^2+(y_i-y_j)^2$, $z_{ij}=z_i-z_j$, and $\Theta(x)$ is the complement of the Heaviside step function. The averages are taken over all pairs of spheres i and j and over $m\cong 25$ shake cycles. We note that, over the range of shaking intensities we have studied, the mean size of vertical displacements during a shake cycle, $\langle |\Delta z_i| \rangle$, is a monotonic, increasing function of the intensity. Figure 9(a) shows that $H(r)$ decreases rapidly to zero with increasing r, and that there is a small decrease in the magnitude of the longitudinal displacement correlations, measured in the transverse direction, as the shaking intensity is increased. The data in Fig. 9(a) give an estimate for the horizontal range over which the spheres

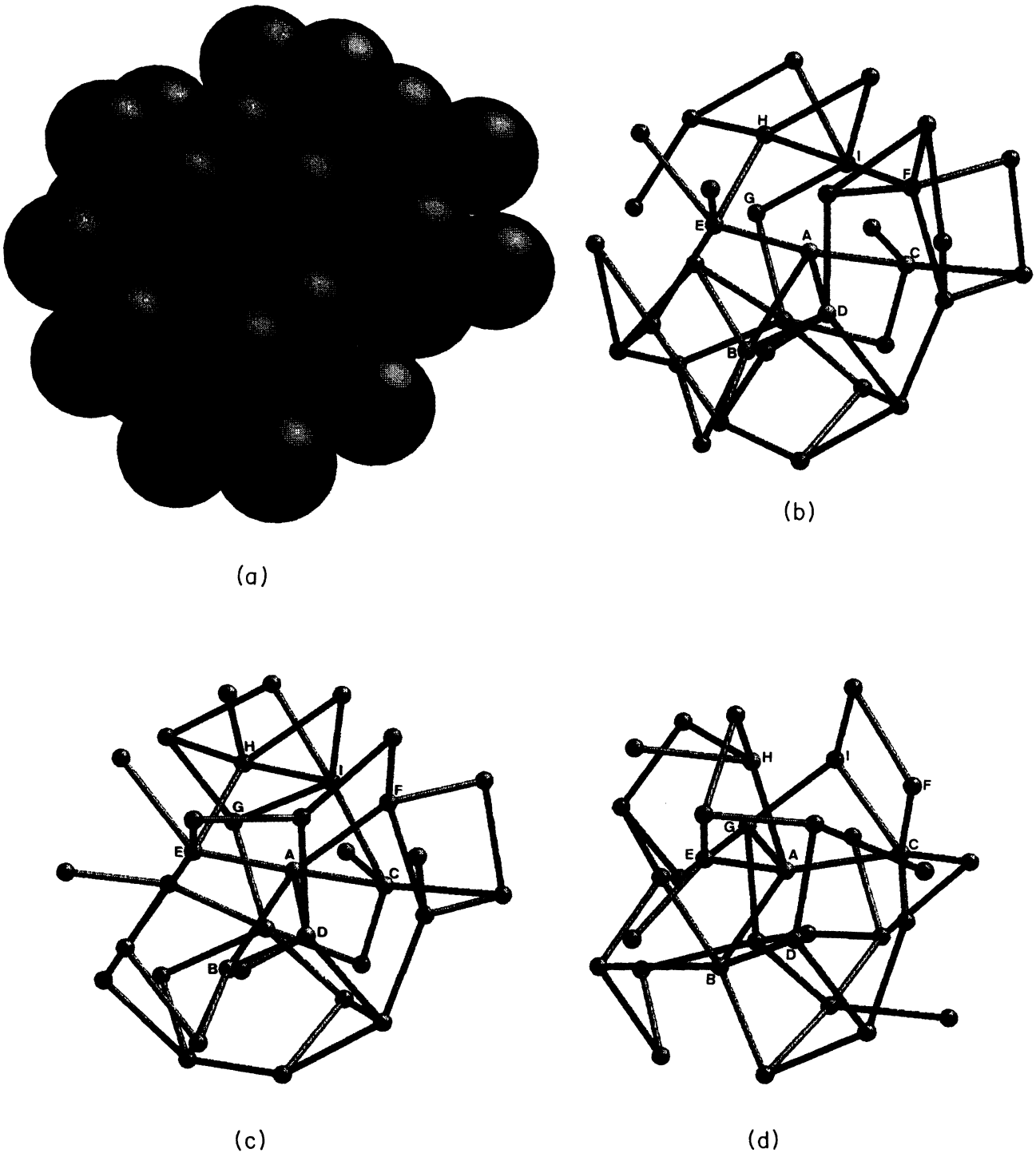

FIG. 7. (a) Three-dimensional representation of a cluster of 35 spheres. The cluster is part of a large assembly of spheres that have been subjected to shaking vibrations with intensity $\epsilon=0.05$. (b) The contact network that corresponds to the cluster of spheres shown in (a). Small balls represent the centers of the packed spheres and rods represent the contacts between them. The centers of the spheres *B*, *C*, *D*, and *E*, which contact the central sphere *A*, have been colored red. Contacts with the spheres that are outside of the cluster have not been shown. (c) The contact network that corresponds to the cluster of spheres that is obtained after the cluster in (a) is subjected to a further shake cycle with intensity $\epsilon=0.05$. (d) The contact network that corresponds to the cluster of spheres that is obtained after the cluster in (a) is subjected to a further shake cycle with intensity $\epsilon=0.5$.

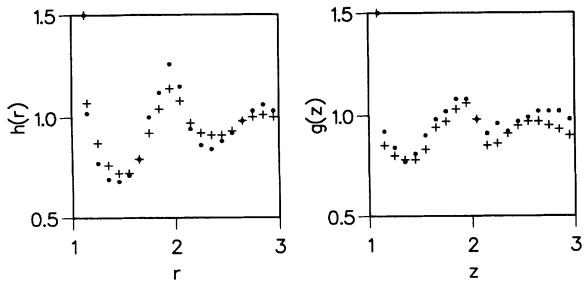

FIG. 8. Pair distribution functions of particle positions $h(r)$ and $g(z)$ for monodisperse hard spheres in the steady-state regime plotted against horizontal displacement r and vertical displacement z. The shaking intensity is $\epsilon=0.05$ (●) and 0.5 (+). The peak heights, which are not shown, have been estimated as $h(1)=6.35(6.20)$ and $g(1)=4.40(4.25)$ for $\epsilon=0.05(0.5)$.

move collectively during a shake cycle, and thus provide a measure of the typical "cluster size" in the transverse direction.

Clearly, during vertical shaking, the motion of a particle is more sensitive to the positions and the motion of those neighbors that are above or below than it is to those that are alongside. Figure 9(b) shows that the correlations of the longitudinal displacements measured in the longitudinal direction are stronger than those measured in the transverse direction, that is, $G(z)$ has a large first peak and, at large displacements, it decreases more slowly than $H(r)$. Also, $G(z)$ depends strongly on the intensity of the vibrations, and, for small ϵ, it has a distinct (negative) minimum at approximately $z=1.3$ sphere diameters. This implies that at these separations, which are typical of vertical particle separations in shallow bridges, many sphere displacements are not strongly correlated, and several of them move in opposite directions; hence this feature is consistent with the slow compression or collapse of shallow bridges. The correlation functions of the transverse components of the sphere displacements are negative at small separations, which is consistent with spheres sliding past each other as they are displaced in the x and y directions.

We conclude from all the above that the size of a typical dynamical cluster, in both longitudinal and transverse directions, decreases with increasing intensity of vibration. This verifies the predictions of the microscopic

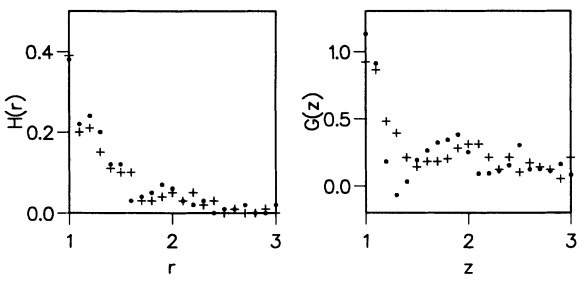

FIG. 9. Correlation functions $H(r)$ and $G(z)$ for the vertical displacements of spheres during a single cycle of the steady-state shaking process plotted against horizontal displacement r, and vertical displacement z. The shaking intensity is $\epsilon=0.05$ (●) 0.5 (+).

model [3], which says that collective (independent-particle) motions predominate for lower (higher) intensities of vibration.

D. The "hole" space

We have concentrated on the static properties and the pair correlations of spheres that form a random-close-packed structure. Equally fundamental, and intimately related, problems concern the nature of the continuous network of empty space, consisting of pores, necks, and voids, etc., which complement the physical structure. In order to investigate the pore space of shaken packings, we have constructed the complex structures formed from overlapping holes. For a close-packed bed of spheres, the overlapping holes are another species of spheres, each of which touches four of the packed spheres. The holes may overlap each other but cannot intersect any of the packed spheres. For a monodisperse close packing, the maximum hole size is approximately the same as the sphere size, and the minimum hole diameter is 0.224 times that of the spheres, corresponding to the hole at the center of a regular tetrahedron formed from four spheres.

Figure 10 shows a small section of the overlapping hole structures for vibrated packings with $\epsilon=0.05$, 0.5, and 1.5, and Fig. 11 shows the corresponding distribution functions for the hole radii. From Fig. 11, it is clear that small-intensity shaking is an efficient method of removing larger holes from the overlapping hole structure, and, therefore, a method for removing large voids from a packing without producing a regular structure. We also note, from Fig. 10, that low-intensity shaking leads to large numbers of isolated holes, and isolated hole pairs, whereas the larger-intensity vibrations create clearly defined strings of connected, overlapping holes. This important feature has clear implications for the transport properties of vibrated beds of particles, and we hope to report on these in more detail at a later date.

E. The surface

In addition to furnishing data on the bulk properties, our simulations can be used to obtain information about the surface of shaken particulate assemblies. Surface measurements are subject to larger uncertainties than bulk measurements because they involve only a fraction of the particles contained in the simulation cell, and also because they are generally more susceptible to system size dependence. For simulations with $L=8$ particle diameters and $N\cong 1300$, we have measured the mean-square surface width $\sigma^2=L^{-2}\sum_i(z_i-z_0)^2$ defined by the spheres i, which have heights z_i and which are the highest spheres in each L^2 vertical columns that have cross sections of one square-sphere diameter. z_0 is the mean height of the bed. All the surfaces that we have examined are smoother than the surface of a sequentially deposited aggregate that has $\sigma^2=0.44\pm0.02$. For $\epsilon\leq 0.5$, the surface width is approximately independent of ϵ and $\sigma^2\cong 0.16\pm0.02$. For larger shaking intensity, σ^2 increases with ϵ, and for $\epsilon=1.5$, $\sigma^2\cong 0.23\pm0.02$. This is in keeping with the qualitative predictions [3] of our model, which state that greater surface roughening arises as a consequence of violent vibrations. We have not been able

to establish the scaling properties of σ^2; however, we have confirmed that these trends are followed by other measures of the surface irregularity. Most notably we have used a Monte Carlo method to investigate the reaction surface for ballistic aggregation with small test particles, which have a diameter of 0.001 sphere diameters—in this case as well, the mean-square width of the reaction surface follows the behavior outlined above.

Other studies of surface roughening [35–37] have concentrated on the scaling regime appropriate to sequential deposition in the presence of noise. Since our current approach is restricted to sizes below the scaling regime, because we incorporate complex and nonsequential reorganization processes, we are unable to compare our results on surfaces with those presented in Refs. [35–37].

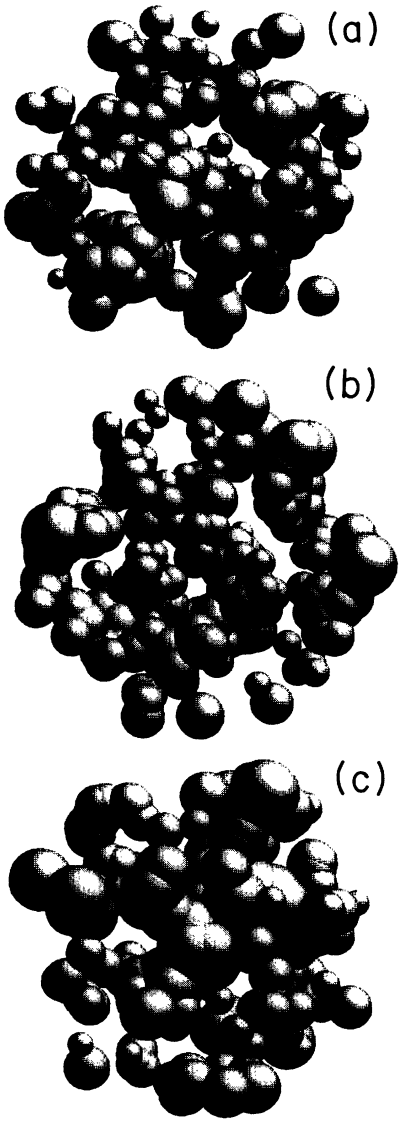

FIG. 10. Sections of the overlapping hole structures that are topologically complementary to the structures formed by the spheres. The shaking intensity is (a) $\epsilon=0.05$, (b) $\epsilon=0.5$, and (c) $\epsilon=1.5$.

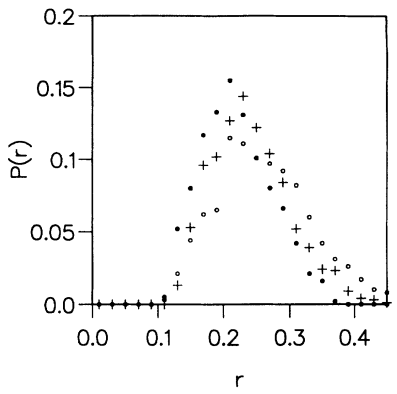

FIG. 11. Distribution functions $F(r)$ for the radii r of the overlapping holes presented in Fig. 10. The shaking intensity is $\epsilon=0.05$ (●), $\epsilon=0.5$ (+), and $\epsilon=1.5$ (○).

However, the results we have presented do provide a quantification of surface roughening in cooperatively restructured packings. We hope to report further on the surface properties of shaken particulate assemblies, as well as the surface-penetration effects, at a later stage.

V. DISCUSSION

In the preceding sections we have shown that our simulations provide direct and meaningful microscopic observations of nonsequentially reorganized granular structures. The simulation technique allows us to observe the packing both internally and nondestructively (which is outside the scope of current experimental techniques), and it therefore provides a unique opportunity to learn about the bulk behavior and the transient responses of granular solids subjected to vibration by focusing on the relaxation mechanisms at the particulate level. Thus our simulation method provides a description that is superior to a continuum description and that provides the basis for a fundamental understanding of realistic (nonsequential) particle dynamics.

The hybrid Monte Carlo method used above allows us to construct, both efficiently and consistently, nonsequential reorganizations of random close packings, but, in so doing, it sacrifices detailed knowledge of the granular dynamics and is unable to look at the effects of the quality and the frequency of the applied vibrations. In this sense, we have not built a model of one particular shaking process from which quantitative data will result, but have designed a working tool to study the qualitative features of shaking and nonsequential processes, in general.

All our simulations have been performed using monodisperse collections of spheres in open systems. It is unlikely that the introduction of a small amount of polydispersity, in either the sizes or the shapes of the particles, would seriously alter our conclusions. However, it is certain that, ultimately, the introduction of variations in the sizes and the shapes of the particles would cause new shaking-induced effects, such as size segregation and the appearance of particularly favorable close packings, to interact with, and probably cloud, the effects that we have observed. Also, we have employed periodic boundary

conditions throughout in order to compensate, at least in part, for the size restrictions that are imposed by our computational limits. It must be emphasized that confining walls and the particle wall interactions play a major role in most powder-handling applications. The extension of our scheme to include the effects of polydispersity, confining walls, as well as other interparticle interactions, represents a primary goal of our future work.

We note that the algorithm, as employed here, does not ensure the homogeneity of bridge nucleation. This is because, in the ordered consolidation in phase 3 of our shake cycle, the packing gradually produces a gap between consolidated and unconsolidated particles. The size of our simulations makes this effect relatively unimportant, but, in larger simulations, the effect can be overcome by incorporating into the consolidation phase a three-dimensional extension of the local shifts that were introduced by Duke *et al.* [4] to ensure homogeneous distribution of bridges in a two-dimensional shaken pile.

The results we have presented establish links between the observed changes of the material properties, which occur as the shaking intensity varies, and the underlying microscopic correlations of the particle positions and displacements. From these results we identify competing roles for the independent-particle and the collective relaxation mechanisms that occur in nonsequentially reorganized random close packings—and verify earlier predictions [3] that independent-particle (collective) effects dominate at high (low) vibration intensity. Contact network measurements show that at high intensities, individual particles are regularly ejected out of their local environments, and, hence, one particle may sample many different environments over a short period of time. In contrast, at low shaking intensities, each particle experiences a slow deformation of its environment during shaking, and the identity of the particles that form its close neighbors remains relatively constant; thus, at these lower shaking intensities it is rare for a particle to make a transition into a totally new environment.

In our packings, the particles that form parts of cooperative structures, such as bridges and arches, are subject to the different rates of change of their local environment caused by different shaking intensities. This leads to nonsequential reorganization behavior which depends, qualitatively, on the shaking intensity. During high-intensity shaking, cooperative structures form and disappear rapidly, so that most of the bridges, etc., that are present in one particular configuration are only one or two generations old. These "immature" bridges have shapes that are those most favored at their formation, and these are, in general, wasteful of space. Thus the packing fraction takes a low value. In the low-intensity regime, the cooperative structures form and then deform, along with their local environment, over several further cycles before they become too tenuous to survive. In this case, a packing may contain bridges that are many generations old ("mature") and that have shapes that are favored by their stability against disruption. This includes shapes that have relaxed downwards and are therefore "flatter"; the result is a higher packing fraction, i.e., a minimization of the void space, and a shift of the hole size distribution to smaller sizes.

According to our definition of a "bridge," several of the spheres that form part of the structure will have a deficit of neighbors, particularly in the downward direction, and, therefore will have low coordination numbers. Thus the mean coordination number of a packing will depend on the density of bridge contacts, and in turn this density will depend on the number density of the bridges and on the mean size of a bridge (i.e., the mean number of spheres that are required to construct one bridge). We can determine the latter from our measurements of $H(r)$; these indicate the lateral extent over which the vertical displacements of the spheres are positively correlated during one shake cycle, and our results show (Fig. 9) that the mean bridge width is quite insensitive to the shaking intensity. Nonzero correlations extend over approximately 1.5 sphere diameters, indicating an average bridge width in the region of 3.0 sphere diameters, for both large and small intensities of vibration.

Given the observed independence of the mean coordination number on ϵ, for $\epsilon \geq 0.25$, we infer that the number density of bridges is approximately constant in this regime. For $\epsilon < 0.25$, the mean coordination number rises, which indicates (since the bridge size stays approximately constant) that the mean number density of bridges *falls*.

We now show the effect of the nature of the collapsed bridges on the resultant packing. For the lowest shaking intensities, the packing includes regions that result from slowly collapsed, mature, and flatter bridges, i.e., bridges that deformed considerably before their contact network was disrupted. We suggest that these are regions of particularly efficient random close packing and therefore cause the mean volume fraction to rise above the value that can be obtained by sequential packing processes. The enhanced short-range correlations of the particle positions (cf. Fig. 8), which we observed for $\epsilon = 0.05$, are consistent with this interpretation. In the high-intensity regime, it is the "immature" and angular bridges that collapse, and the aftermath of such collapses is not distinguishable from a sequentially deposited structure, with smaller short-range correlations in particle positions and lower packing fractions. The above thus illustrates (via the specific mechanism of bridge collapse) the point [3] that, at low intensities of vibration, collective reorganization of particles (and the consequent slow rearrangement of particle bridges) will lead to the efficient filling of voids, and the converse.

In conclusion, then, we have presented a detailed study of the microscopic processes at work in the interior of a vibrated granular pile. We have investigated the bulk structure, by analyzing the behavior of the volume fraction and the distribution of coordination numbers as a function of the shaking intensity. We have also presented a detailed study of the contact networks and their autocorrelation functions before and after vibration, and have shown that earlier predictions [3,8] regarding the roles of independent-particle and collective relaxation mechanisms are verified. The spatial correlations in the pile after vibration have been investigated by examining the

pair-correlation functions of particle positions, and the distributions of voids, as a function of intensity, which provide valuable clues to the static as well as to the transport properties, with particular reference to the important issue of bridge formation and collapse. Finally, we have shown directly the dynamical behavior of grains submitted to vibration, by examining the displacement correlation functions as a function of intensity and demonstrating that the slow motion of clusters predominates at lower intensities, relative to the motion of independent particles, and the converse. We look forward greatly to experimental verification of this rich array of theoretical [3,4,8,9] results, which our present work in its detail has brought within reach of current experimental techniques [38].

ACKNOWLEDGMENTS

We thank Richard Needs, Mike Cates, and Malcolm Grimson for useful comments on the manuscript.

*Present address.

[1] R. A. Bagnold, Proc. R. Soc. London Ser. A **225**, 49 (1954); **295**, 219 (1966).
[2] R. L. Brown and J. C. Richards, *Principles of Powder Mechanics* (Pergamon, Oxford, 1966).
[3] Anita Mehta, in *Correlations and Connectivity; Geometrical Aspects of Physics, Chemistry and Biology,* edited by H. E. Stanley and N. Ostrowsky (Kluwer, Dordrecht, 1990), pp. 88–108.
[4] T. A. J. Duke, G. C. Barker, and Anita Mehta, Europhys. Lett. **13**, 19 (1990).
[5] Anita Mehta and S. F. Edwards, Physica A **168**, 714 (1990).
[6] L. P. Kadanoff *et al.*, Phys. Rev. A **39**, 6524 (1989).
[7] H. M. Jaeger *et al.*, Europhys. Lett. **11**, 619 (1990).
[8] Anita Mehta, R. J. Needs, and S. Dattagupta (unpublished).
[9] Anita Mehta and G. C. Barker, Phys. Rev. Lett. **67**, 394 (1991).
[10] G. W. Baxter *et al.*, Phys. Rev. Lett. **62**, 2825 (1989).
[11] H. M. Jaeger, C. Liu, and S. R. Nagel, Phys. Rev. Lett. **62**, 40 (1989).
[12] G. A. Held *et al.*, Phys. Rev. Lett. **65**, 1120 (1990).
[13] Ory Zik and Joel Stavans (unpublished).
[14] M. J. Vold, J. Colloid Interface Sci. **14**, 158 (1959).
[15] W. M. Visscher and M. Bolsterli, Nature **239**, 504 (1972).
[16] R. Jullien and P. Meakin, Europhys. Lett. **4**, 1385 (1987).
[17] T. A. Witten and L. M. Sander, Phys. Rev. Lett. **47**, 1400 (1981).
[18] J. Bridgwater, Powder Technol. **15**, 215 (1976).
[19] D. S. Parsons, Powder Technol. **13**, 269 (1977).
[20] J. C. Williams and G. Shields, Powder Technol. **1**, 134 (1967).
[21] C. S. Campbell and C. E. Brennan, J. Fluid Mech. **151**, 167 (1985).
[22] O. R. Walton, Int. J. Eng. Sci. **22**, 1097 (1984).
[23] J. D. Bernal, Proc. R. Soc. London, Ser. A **280**, 299 (1964).
[24] A. Rosato *et al.*, Phys. Rev. Lett. **58**, 1038 (1987).
[25] W. Soppe, Powder Technol. **62**, 189 (1990).
[26] P. A. Cundall and O. D. L. Strack, Geotechnique **29**, 47 (1979).
[27] See, e.g., *Tribology in Particulate Technology,* edited by M. J. Adams and B. J. Briscoe (Hilger, Bristol, 1987).
[28] G. W. Baxter and R. P. Behringer, Phys. Rev. A **42**, 1017 (1990).
[29] P. K. Haff, J. Fluid Mech. **134**, 401 (1983).
[30] J. T. Jenkins and S. B. Savage, J. Fluid Mech. **130**, 187 (1983).
[31] R. Jackson, in *Theories of Dispersed Multiphase Flow,* edited by R. Meyer (Academic, New York, 1983).
[32] G. C. Barker and M. J. Grimson, J. Phys. Condens. Matter **1**, 2779 (1990).
[33] J. G. Berryman, Phys. Rev. A **27**, 1053 (1983).
[34] G. C. Barker (unpublished).
[35] S. F. Edwards and D. R. Wilkinson, Proc. R. Soc. London, Ser. A **381**, 17 (1982).
[36] M. Kardar, G. Parisi, and Y. C. Zhang, Phys. Rev. Lett. **56**, 889 (1986).
[37] R. Jullien and R. Botet, Phys. Rev. Lett. **54**, 2055 (1985).
[38] S. K. Sinha (private communication).

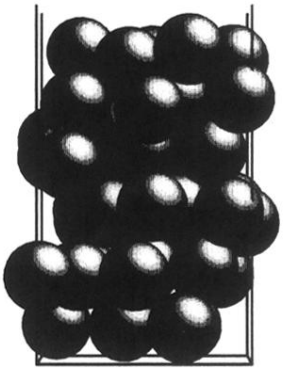

FIG. 1. Schematic diagram of the geometry of the simulation. Hard particles form a periodic bed above an impenetrable base: the diagram shows the primary simulation cell, which is repeated in two perpendicular directions.

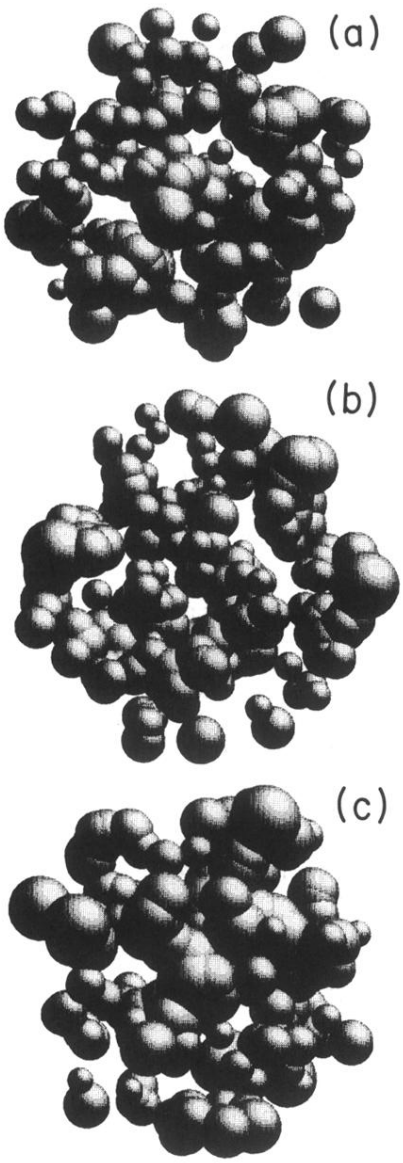

FIG. 10. Sections of the overlapping hole structures that are topologically complementary to the structures formed by the spheres. The shaking intensity is (a) $\epsilon=0.05$, (b) $\epsilon=0.5$, and (c) $\epsilon=1.5$.

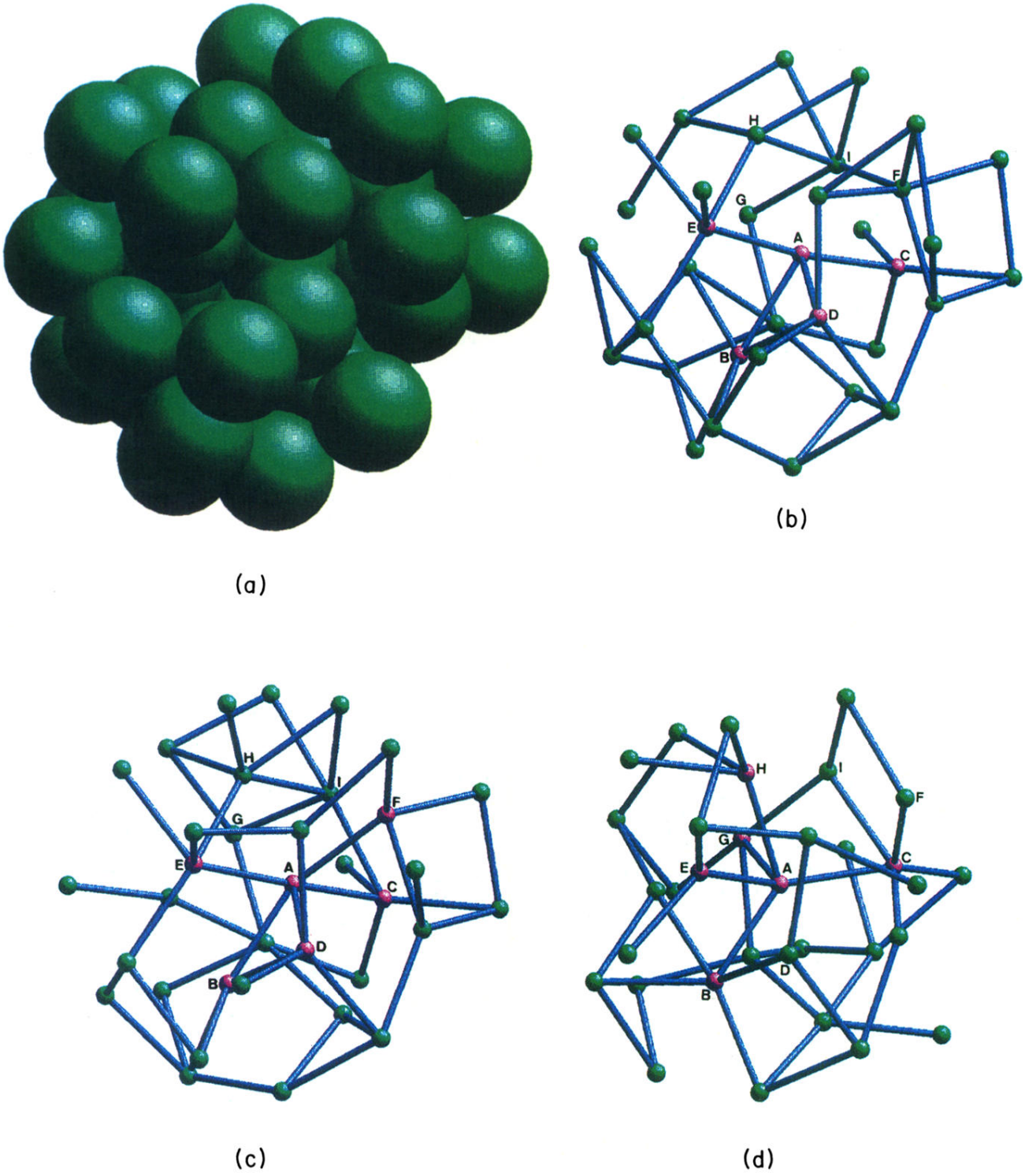

FIG. 7. (a) Three-dimensional representation of a cluster of 35 spheres. The cluster is part of a large assembly of spheres that have been subjected to shaking vibrations with intensity $\epsilon=0.05$. (b) The contact network that corresponds to the cluster of spheres shown in (a). Small balls represent the centers of the packed spheres and rods represent the contacts between them. The centers of the spheres *B*, *C*, *D*, and *E*, which contact the central sphere *A*, have been colored red. Contacts with the spheres that are outside of the cluster have not been shown. (c) The contact network that corresponds to the cluster of spheres that is obtained after the cluster in (a) is subjected to a further shake cycle with intensity $\epsilon=0.05$. (d) The contact network that corresponds to the cluster of spheres that is obtained after the cluster in (a) is subjected to a further shake cycle with intensity $\epsilon=0.5$.